Performance of auxiliary wind propulsion for merchant ships using a kite

Peter Naaijen, Delft University of Technology & **Vincent Koster**, Delft University of Technology

SUMMARY
The current paper describes a performance study of auxiliary wind propulsion for merchant ships by means of a traction kite. It is not considering practical design aspects of such a system and therefore not concluding on practical feasibility, rather it gives an indication of how much fuel can be saved in various environmental conditions, assuming a working system.
A model is described for calculating the delivered traction force of a kite. Depending on the apparent wind direction and wind speed, this kite force will cause a drift angle of the ship resulting in additional resistance. This effect, taken into account by simultaneously solving the force balance in longitudinal and lateral direction and the yaw balance appears to be small.
Finally, in order to calculate the effect of auxiliary kite propulsion on the fuel consumption, the performance in off-design conditions of the existing engine and propeller is considered.
Results of a case study are presented showing the relative fuel saving as a function of wind speed and wind direction relative to the sailing direction.

1 INTRODUCTION

These days, while oil price records being broken is the order of the day, renewed interest in sustainable energy solutions for transportation results in interesting alternatives that reduce fossil fuel consumption. The direct environmental and (with today's oil prices) financial benefits of saving fossil fuel is obvious. Besides, indirect benefits result from authority regulations that tend to increase the pressure on shipping industry to reduce emissions: the main focus of IMO's regulations on ship emissions at the moment is to tighten up current MARPOL Annex VI limits on sulphur oxide (SOx), nitrogen oxide (NOx) and other harmful gases and the European Commission confirmed recently that it will propose bringing CO_2 emissions from ships into the European Union's emissions trading scheme (ETS). [1] Shipping is the most energy-efficient mode of transport which is probably why the sector has got away with doing very little to reduce emissions until now. The fact that shipping (responsible for transporting more than 90 % of world trade) accounts for approx. 5 % of global CO_2 emissions [1] is more and more considered to be a good reason to change this: There seems to be a lot to gain.
One way to achieve this is to reintroduce wind power. Having some advantages compared to conventional sails, a traction kite propulsion system for commercial ships is an interesting concept which is being worked on by various parties in industry. [2][3] Though initially received with some scepticism , the idea is getting more and more serious attention from ship owners. Another concept that is being developed is the so-called laddermill sailing system that combines the ability of a kite to deliver direct traction force at following wind conditions and produce electrical power at head wind conditions [15].
This paper considers the specific concept of a high performance (high lift to drag ratio kite, similar to the ones used in sports like kite surfing and kite sailing [4]) for traction force generation. Attached to a single tow line via a steering gondola, these kites can be actively controlled in order to create high flying speeds resulting in high traction force. Figure 1 depicts such a kite-ship system.

Figure 1, Ship with kite [2]

Compared to more conventional wind propulsion by sails, there are some benefits involved with applying kites:

- a kite can be actively controlled in order to create its own flying speed thus increasing its apparent wind speed and the traction force: more traction power can be created with less 'sail' area this way.
- due to the fact that a kite can fly at higher altitudes it is exposed to higher wind speed
- due to the low attachment point of the tow line the roll heeling moment is considerably smaller
- there are no masts taking deck space

In the next sections a way to estimate the kite traction force is described. The effect of the towing force by the

kite on both the hull hydromechanics and the existing propulsion installation is discussed and results in terms of relative fuel saving following from a case study are presented.

2 KITE TRACTION

2.1 INTRODUCTION

A kite can be considered as a wing surface which enables the application of existing aerodynamic concepts: the resulting force acting on a kite is determined by calculating lift and drag on a 3D wing surface being governed by relative wind speed and angle of attack. The main assumption for the model is instantaneous equilibrium between the direction of the tow line and the direction of the resultant aerodynamic force on the kite. For a kite, this equilibrium is depending on its position in space which will be described using the so-called flight envelope (FE). The apparent wind speed, experienced by the kite is a combination of true wind and the kite's own flying speed. (For the time being the forward speed of the ship which also provides a wind component entering the FE is not explicitly considered. It is introduced later on.)
Depending on the position, the kite will develop its flying speed in such a way that the resulting force is parallel to the tow line. It's the main purpose of the kite performance calculation to determine this equilibrium speed and the resulting towing force.

2.2 FLIGHT ENVELOPE

The set of possible positions in space of a kite, attached to a tow line with length *r*, is described by a quarter sphere with radius *r*, which is called the flight envelope (FE). See Figure 2 where the direction of the true wind is indicated. True wind speed is defined by *W*. Point *F* is the attachment point of the tow line. The half circle *LUR* is called the edge of the FE. *P* is the centre of the so-called power zone. When assuming uniform inflow over the altitude in the FE, *P* is the point where the highest speed and traction of the kite are obtained. (The effect of a boundary layer for the wind speed in which wind speed increases with altitude is discussed later on.) All half circles parallel to *LUR* are called iso-power lines: kite speed and traction are constant on these lines. All circle segments from *P* to the edge are iso-gradient lines: the gradient of speed and power has a constant maximum value on these lines.
The position of the kite within the FE, indicated by *K* is described by two angles (See Figure 2):
- θ is the inclination of the tow line *FK* with respect to the line *FP*
- Φ is the inclination of the plane *FKP* with respect to the horizontal plane

In order to describe the flying direction of the kite, a kite reference system x_K, y_K, z_K is defined having its origin at *K*. The x_K axis is tangential to the iso-power line through *K* pointing from *L* to *R*, while the y_K axis is tangential to the iso-gradient line through *K* pointing towards *P*. The z_K axis is parallel to the tow line, pointing outwards the FE.
γ is the angle between the flying direction of the kite and the positive x_K axis. See Figure 3 showing a top view (looking in negative z_K direction) on the kite.

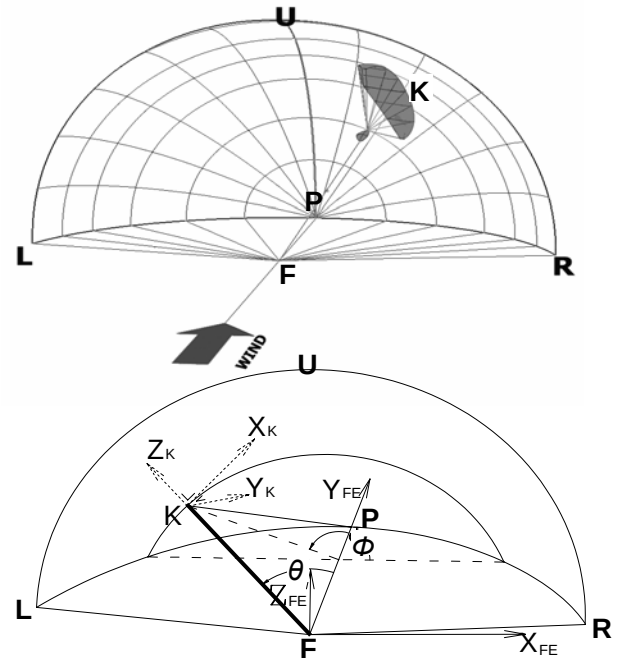

Figure 2, Flight Envelope (FE)

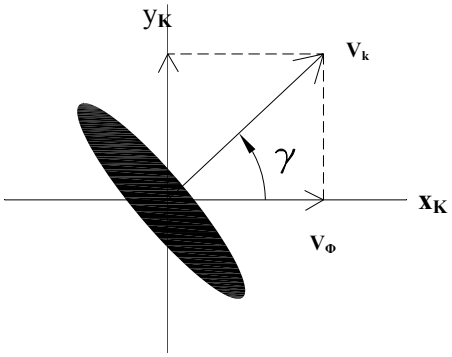

Figure 3, Kite in projected plane of FE

Having defined how the kite's position and flying direction are described, this definition is used now to formulate the apparent wind experienced by the kite.
First, the apparent wind is split up into a part tangential to the FE (v_t) which is a combination of tangential velocities $v_{t\text{-}x}$ and $v_{t\text{-}y}$ in x_K and y_K direction respectively, and a radial part parallel to the tow line in the z_K direction ($v_{r\text{-}z}$)
The tangential velocity is caused by a combination of true wind and kite speed. The part due to the kite speed can be split up into a part tangential to the iso-power lines in the

direction of x_K ($v_{x\text{-}k}$) and a part tangential to the iso-gradient lines in the direction of y_K ($v_{y\text{-}k}$). In y_K direction, there is a contribution by the true wind ($v_{y\text{-}w}$) as well. With the above mentioned definitions, the following formulae for these velocities can be found:

$$v_{t-y} = -r\dot{\theta} + W\sin(\theta) = v_{y-k} + v_{y-w} \quad (1)$$

$$v_{t-x} = -r\sin(\theta)\cdot\dot{\phi} = v_{x-k} \quad (2)$$

Combining these two contributions to the total tangential velocity yields:

$$v_t = \sqrt{(v_{t-x})^2 + (v_{t-y})^2} \quad (3)$$

For the flying speed v_k and direction γ of the kite follows:

$$v_k = \sqrt{{v_{y-k}}^2 + {v_{x-k}}^2} \quad (4)$$

$$\gamma = \arctan\left(\frac{v_{y-k}}{v_{x-k}}\right) \quad (5)$$

The radial velocity is caused by true wind only:

$$v_{r-z} = W\cos(\theta) \quad (6)$$

With the above defined velocities, a formula for the total relative velocity v_{rel} and the angle of attack α experienced by the kite can be derived: (See Figure 4 which depicts a cross section of the kite and the involved angle of attack.)

$$v_{rel} = \sqrt{(v_t)^2 + (v_{r-z})^2} \quad (7)$$

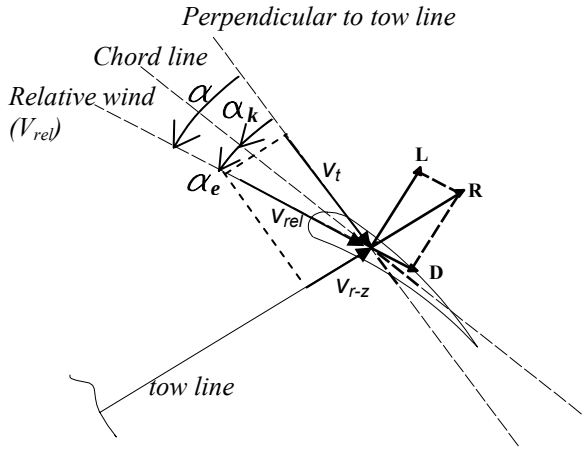

Figure 4, Kite Angle of Attack

$$\alpha = \arctan\left(\frac{v_{r-z}}{v_t}\right) \quad (8)$$

To find the *effective* angle of attack, α_e, the angle at which the kite is attached to the tow line, α_k, has to be subtracted from α. (Figure 4)

$$\alpha_e = \alpha - \alpha_k \quad (9)$$

Lift and Drag

To determine the resulting force on the kite, first lift and drag of the 2D airfoil are determined. Corrections to this 2D lift and drag coefficients are made in order to take into account 3D induced drag and the curvature of the kite. Furthermore some additional contributions to the drag are considered which take into account line drag, inlet drag, and drag due to irregularities and surface roughness.

2D lift and drag coefficients are calculated by the free available panel method program XFOIL by Drela & Youngren [5]. The inviscid flow calculated by the program is constructed by a superposition of three potential flows being the free stream, a flow created by a vortex sheet on the airfoil surface and a source sheet on the airfoil surface and wake.

The viscous part of the solution resulting in frictional resistance is described by boundary layer shape parameter equations. For a detailed description of XFOIL reference is made to Drela & Youngren [5] and Drela [6].

The obtained 2D lift and drag coefficients have to be corrected in order to include 3D effects. This is done based on Prandtl's lifting line theory assuming elliptical lift distribution over the wing span.

The fact that a kite has a certain span wise curvature will also effect the lift of the whole kite. Resolving the lift force perpendicular to the curved kite into the Z_K direction results in the following formulation for the lift on the curved kite according to Lingard [8]: (See Figure 5).

$$C_{L,c} = C_L\cos^2(\zeta) \quad (10)$$

where:

C_L = 3D Lift coefficient of straight wing

$C_{L,c}$ = 3D Lift coefficient of curved wing

ζ = angle of curvature (See Figure 5.)

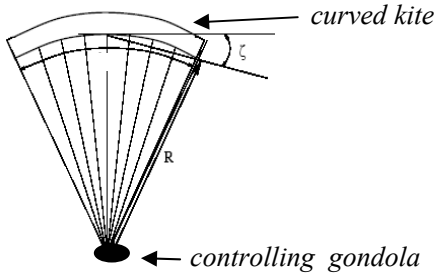

Figure 5, lines between gondola and kite

The lines between steering gondola and kite, where the speed is assumed to equal the speed of the kite itself, appear to generate a considerable amount of drag. The drag coefficient of all these lines together can be determined using the formulation of Prakash [9]:

$$C_{D,l} = \frac{n \cdot R \cdot d \cos^3(\alpha_l)}{S} \qquad (11)$$

where:
$C_{D,l}$ = drag coefficients of lines between gondola and kite
n = number of lines
R= length of lines between gondola and kite
d = diameter of individual lines
α_l = angle of attack between relative speed and kite line
S = kite area

According to Prakash [9] the number of lines depends on the kite aspect ratio as follows:

$$n = 8 + 16AR \qquad (12)$$

The diameter of the individual lines between gondola and kite is chosen such that their total cross sectional area equals that of the tow line between gondola and ship.
For determining the line drag the part of the tow line underneath the gondola and the part between gondola and kite are considered separately. For the lower part it appeared that even when taking into account a line drag coefficient of 3, the drag of the tow line did not exceed 1% of the total drag (partly because the speed of the tow line itself is low). Therefore the lower tow line drag is neglected. (It must be noted however that an increase in line drag can be expected due to vortex induced vibrations which is not taken into account here.)
Other additional drag coefficients come from the air inlet, and surface irregularities and surface roughness. The air inlet is an opening at the nose of the kite enabling air flow into the inflatable kite. Approximations for drag coefficients of these components given by Prakash [9] have been used.

2.3 EQUILIBRIUM VELOCITY

As mentioned, the key assumption of the presented approach to calculate the kite traction is the resultant force on the kite being parallel to the tow line. When assuming that the Reynolds number (based on which the 2D lift and drag coefficients are calculated) is independent of the instantaneous relative kite velocity v_{rel} and as a consequence independent of the position of the kite in the FE, the Lift to Drag ratio (L/D) is also independent of the kite position. This means that the direction of the resultant kite force depends on the angle of attack only. With a known L/D, the required angle of attack for which the resultant kite force is parallel to the tow line is easily determined and also independent of the kite position.
Equation (8) gives the relation between angle of attack and radial and tangential relative velocity of the kite. The radial velocity $v_{r\text{-}z}$ is a result of true wind only (equation (6)) and depends on the position of the kite on the FE. The tangential velocities $v_{t\text{-}y}$ and $v_{t\text{-}x}$ however are strongly dependent of the kite's own speed in terms of $\dot{\phi}$ and $\dot{\theta}$. So for a given flying direction γ and a given position on the FE (defined by ϕ and θ), the required angle of attack for which the resultant force on the kite is indeed parallel to the tow line can be obtained by tuning the kite's own speed in terms of $\dot{\phi}$ and $\dot{\theta}$:
By combining equations (1), (2) and (5) $\dot{\theta}$ can be expressed as follows:

$$\dot{\theta} = -\sin(\theta) \cdot \dot{\phi} \tan(\gamma) \qquad (13)$$

By substituting equation (13) and equations (1) and (2) in the expression for the angle of attack (8), a quadratic equation for $\dot{\phi}$ can be obtained:

$$\dot{\phi}^2 \left(r^2 \sin^2(\theta) \cdot \left(1 + \tan^2(\gamma)\right)\right) + \dot{\phi}\left(2r \sin(\theta) \tan(\gamma)\right) = -W^2 \sin^2(\theta) + \left(\frac{W \cos(\theta)}{\tan(\alpha)} \right)^2 \qquad (14)$$

Having solved $\dot{\phi}$ from equation(14), $\dot{\theta}$ follows from equation (13).
Knowing the kite velocities the instantaneous relative velocity v_{rel} of the kite is known which enables the calculation of the resultant force on the kite from the lift and drag force:

$$L = \tfrac{1}{2} \rho v_{rel}^2 S \cdot C_L \qquad (15)$$

$$D = \tfrac{1}{2} \rho v_{rel}^2 S \cdot C_D \qquad (16)$$

As mentioned calculation of lift and drag coefficients is based on a constant Reynolds number (independent of location in the FE and) independent of the instantaneous relative velocity of the kite. Therefore the lift to drag ratio is also independent of the location on the FE and only depending on the angle of attack. The angle α_k between kite cord line and tow line has been chosen such that the angle of attack for which the resultant force is parallel to the tow line is giving the maximum lift to drag ratio. For the kite considered during the case study that will be described in the last paragraph, this L to D ratio amounts to 3.5.

2.4 THE FLIGHT ENVELOPE ON THE SHIP

As mentioned, one of the benefits of a kite is that its relative velocity can be increased by actively maneuvering it on a desired track on the FE.

Such a track could be an orbit shaped as depicted in Figure 6.

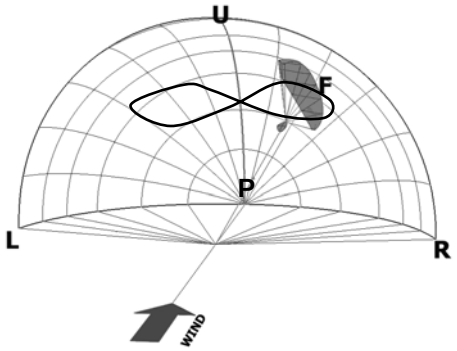

Figure 6, possible kite track on FE

When a certain track is prescribed, total relative kite velocity and traction force at a finite number of points on the track can be determined. The average traction force and its direction can be calculated by a time integration over the chosen orbit. In the present study an orbital shape as depicted in Figure 6 is considered.

In case of a kite towing a ship, the wind that enters the FE (being called 'true' wind until now) is in fact a combination of true wind and wind created by the ship's own speed. In general the direction of these two will not coincide. The FE is positioned on the ship in such a way that its edge is perpendicular to the direction of combined true wind and ship speed at the average flying altitude of the kite. As the kite's flying altitude is supposed to be within the so-called surface layer of the atmosphere, where the occurring wind is dominated by pressure differences and no geotropic winds occur, the variation of wind speed with altitude can be expressed by a logarithmic profile (Troen [7]):

$$W(z) = C_{\log} \ln\left(\frac{z}{z_0}\right) \qquad (17)$$

where:
$W(z)$ = Wind speed at altitude z above (sea) surface

$$C_{log} = \frac{u_{ref}}{\ln\left(\frac{z_{ref}}{z_0}\right)}$$ where:

u_{ref} = known wind speed at reference level
z_{ref} = reference level (10 m)
z_0 = surface roughness (depending on wave height)

Figure 7 depicts a top view on ship and FE for a bow quartering wind condition. Depending on the direction of the apparent wind with respect to the sailing direction, a certain range of horizontal kite positions can be defined resulting in a traction force having a component in the ship's sailing direction. Taking into account the fact that the practical boundaries of the 'accessible area' of the kite are a bit off the edge of the FE, this range is indicated by the hatched area in Figure 7.

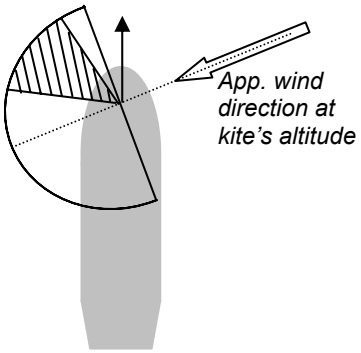

Figure 7, FE on ship for bow quartering wind

Concerning the vertical position of the kite orbit, an optimum can be found resulting in the highest mean traction force in the ship's sailing direction.
This optimum flying altitude is governed by:

- the variation of traction force over the FE
- the variation of wind velocity over altitude
- variation of horizontal traction force with inclination of tow line

To assess the effect of the flying altitude on the kite force in the direction of the forward speed X_{kite}, and to find the optimum flying altitude in terms of maximum X_{kite}, simulations of the kite, flying along an orbital track, have been made for various flying altitudes during a case study. (Details about this case study are presented later on.) For three different towing line lengths, 150 m, 350 m and 550 m and three different wind speeds, the traction force in the direction of the forward ship speed (time-averaged over one revolution on the orbit) has been calculated for various flying altitudes. Results for a towing line length of 150 m are presented in Figure 8.

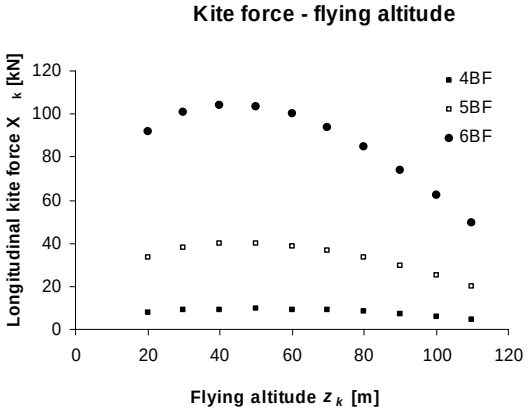

Figure 8, Kite force as a function of flying altitude (for line length = 150 m)

It appears that the altitude at which maximum forward towing force occurs amounts to 27 to 33 % of the towing line length, slightly decreasing with increasing wind speed.
Above presented results are for a wind direction of 0 degrees off the stern. Similar calculations have been made for different wind directions resulting in optimum flying altitudes in the same range.

3 PERFORMANCE PREDICTION

3.1 INTRODUCTION

In the following the kite forces that have been determined are considered as external forces acting on the ship. There are several ways in which this external force effects the performance and with it the fuel consumption of the ship. Basically there are two effects that will be addressed:

- Due to the thrust provided by the kite, the existing propulsion installation will be operated at off-design situations. The performance of propeller and main engine in combination with a kite will be considered in order to determine the fuel consumption.
- In addition to a kite force component in the direction of the forward speed, there will in general also be a component perpendicular to this, resulting in a side force and yawing moment. The resulting drift angle of the ship and rudder angle needed to ensure lateral force balance and yaw balance will effect the resistance of the ship.

3.2 ENGINE AND PROPELLER

As a result of the additional towing force by the kite, less thrust is required from the propeller. Assuming that the ship's forward speed is kept constant, a formulation is given here for determining the propeller loading and corresponding engine power and fuel consumption for this off-design condition.
The force required from the propeller follows from the longitudinal force balance (equation (25)):

$$X_{prop} = R - X_{kite} - X_i \tag{18}$$

Following Kleinwoud & Stapersma [10] for one specific forward speed U, X_{prop} can be written as:

$$X_{prop} = c_1 \cdot U^2 \tag{19}$$

where c_1 is a speed dependent factor:
$c_1 = \left(R - X_{kite} - X_i\right) / U^2$

Using the wake fraction this becomes:

$$X_{prop} = c_1 \cdot \left(\frac{v_A}{1-w}\right)^2 \tag{20}$$

where:
v_A = advance velocity at the propeller
w = wake factor

Taking into account thrust deduction, the required propeller thrust is equal to:

$$T_{prop} = \frac{X_{prop}}{(1-t)} = \frac{c_1 \cdot v_A^{\,2}}{(1-t)\cdot(1-w)^2} = c_8 \cdot v_A^{\,2} \tag{21}$$

where:
t = thrust deduction fraction

$$c_8 = \frac{c_1}{(1-t)\cdot(1-w)^2}$$

For the non-dimensional thrust coefficient follows:

$$K_{T_{prop}} = \frac{c_8 v_A^{\,2}}{\rho n^2 D^4} = \frac{c_8}{\rho D^2} \cdot J^2 \tag{22}$$

where:
ρ = density of water
n = number of propeller revolutions per second
D = propeller diameter
J = advance ratio: $J = \frac{v_A}{nD}$
So the non-dimensional thrust has been expressed by a quadratic function of the advance ratio J. Using the propeller open water diagram J can be solved by matching the propeller's open water K_T value and the above deduced $K_{T_{prop}}$.
The corresponding torque coefficient is found from the open water K_Q curve.
Taking into account the relative rotative efficiency η_R and the transmission efficiency η_{TRM} finally the engine brake power can be found:

$$P_B = \frac{2\pi D^5}{\eta_R \cdot \eta_{TRM}} \cdot K_Q \cdot n^3 \tag{23}$$

The fuel consumption follows from the brake specific fuel consumption $BSFC$ (which is given for the considered engine) and the required brake power.

3.3 HYDROMECHANICS OF THE HULL

Figure 9 defines the involved forces, moments, velocities and angles involved in case of a partly kite-propelled ship sailing with a certain steady drift angle β.

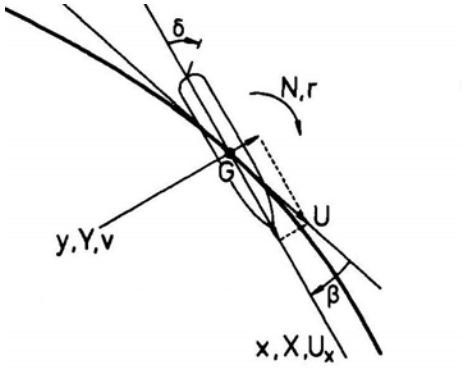

Figure 9, Definition of hydromechanic forces

Writing the hydromechanic hull and rudder forces and moments in terms of the usual maneuvering coefficients neglecting third and higher order terms, the following formulations yield for the horizontal force and moment balance:

lateral force balance:

$$Y_{kite} + Y_v v + Y_\delta \delta + Y_{\delta\delta}\delta^2 = 0 \qquad (24)$$

longitudinal force balance:

$$X_{kite} + X_{prop} - R + X_{vv}v^2 + X_{\delta\delta}\delta^2 + X_{v\delta}v\delta = X_{kite} + X_{prop} - R + X_i = 0 \qquad (25)$$

yaw balance:

$$N_v v + N_\delta \delta + N_{\delta\delta}\delta^2 + Y_{kite} \cdot x_{kite} = 0 \qquad (26)$$

where:

v = lateral ship speed

δ = rudder angle

subscripts v and δ denote derivatives to lateral speed and rudder angle

Y, X, and N = lateral force, longitudinal force and yaw moment where subscript *kite* denotes forces induced by the kite.

X_i = induced longitudinal force due to rudder angle and drift: $X_i = X_{vv}v^2 + X_{\delta\delta}\delta^2 + X_{v\delta}v\delta$

X_{prop} = longitudinal force provided by propeller

R = calm water ship resistance

x_{kite} = distance between kite attachment point and ship's centre of rotation (COG)

From the equations for the lateral force balance and yaw balance, v and δ can be found by simultaneously solving these equations. Knowing these, the required propeller force X_{prop} can be found from the longitudinal force balance. However, rudder force coefficients N_δ and $N_{\delta\delta}$ are dependent of the flow velocity at the rudder which in its turn depends on the increase of flow velocity due to the propeller. The latter is governed by the thrust that has to be delivered by the propeller and therefore there is a coupling between the equation for the longitudinal force balance (25) and those for the lateral force and horizontal moment balance, (24) and (26). The effect of the lateral ship speed, v, on the propeller performance (among others the propeller producing a side force in an inclined incoming flow) has been ignored.

Obviously the hydromechanic yaw moment on the hull ($N_v v$) and the yaw moment induced by the kite ($Y_{kite} \cdot x_{kite}$) have opposite directions. The difference will have to be compensated by the rudder which will also result in extra resistance. During the case study described in the last paragraph it appeared that the optimal position of the kite attachment point (for which a minimum rudder angle is required to ensure yaw balance) is as far forward on the bow as possible.

3.4 APPLICATION OF A 500 m^2 KITE TO A 50.000 DWT TANKER

In this section the above described theory is applied to a 50.000 DWT tanker powered by a 12000 kW diesel engine and a 500m^2 kite. One reason for choosing a tanker with a low forward speed (15,5 kn) is that such a ship is likely to benefit the most from wind propulsion as the apparent wind direction will be relatively more from the stern than will be the case for a faster ship type. Another reason is that extensive model experiments have been carried out by Journee [11] at the Delft University Ship Hydromechanics Laboratory in the late 60's with a model of this particular ship providing all the necessary hydromechanic data on the hull to perform the performance prediction calculations. The ship was originally equipped with a steam turbine. For this study an equivalent diesel engine was considered.

A more detailed description of the ship used for the case study can be found in [12].

For the cross sectional shape of the kite a similar airfoil shape was used as is often applied for kite surfing which is a NACA 4415, depicted in Figure 10. A wing with an area of 500 m^2 and an aspect ratio of 4 attached to a towing line of 350 m length was adopted having an elliptical cord length distribution over the span.

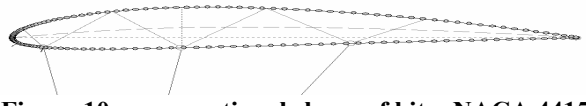

Figure 10, cross sectional shape of kite: NACA 4415

3.5 RESULTS, DISCUSSION AND CONCLUSIONS

The result of the case study described in the previous section is presented as a polar diagram of relative fuel saving in **Figure 11**. The angular axis represents the true wind direction from the bow. The radial distance from the

origin represents the fuel consumption as a percentage of the fuel consumption as it would be without using the kite. The different lines represent different wind speeds as indicated in the legend. In all calculated conditions wind resistance and added resistance in waves is included. (Wind resistance is calculated according to Isherwood [13]. For added resistance in waves model test results have been used [11].)

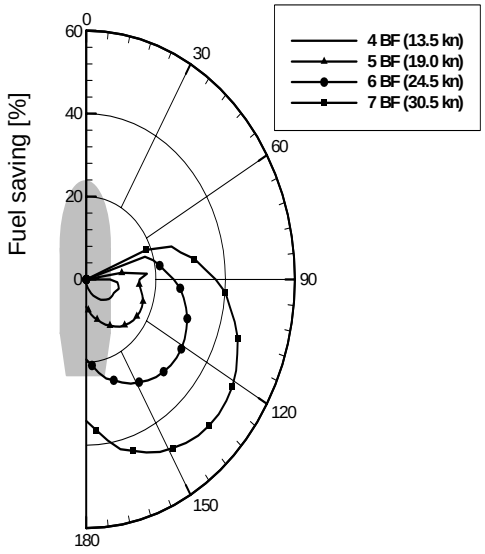

Figure 11, Relative fuel saving, 350 m line length

For upwind conditions, the kite cannot be operated as the apparent wind direction simply leaves no accessible area where the kite is able to fly a prescribed orbit resulting in a propulsive force. (See Figure 7.) This is why no fuel saving is obtained for upwind true wind directions.
As can be seen, fuel saving rapidly increases with wind speed. For a wind speed of Beaufort 6 the fuel saving amounts to up to 32 % while for Beaufort 7 savings of 50% are achieved.

Drift induced resistance and unfavorable off-design operation of the existing propulsion installation were expected to result in a lower relative fuel saving than relative propulsion force contribution by the kite. However, this did not appear from the case study. Relative fuel saving even slightly exceeds the relative propulsion force by the kite in some cases. An explanation for this can be found in the open water propeller efficiency. See Figure 12 which shows the open water propeller characteristics for the case ship.
The design point (without kite) and the off design condition (with kite) for maximum kite propulsion force at Beaufort 7 are indicated. The figure shows that the open water efficiency changes from 0.59 to 0.63, an

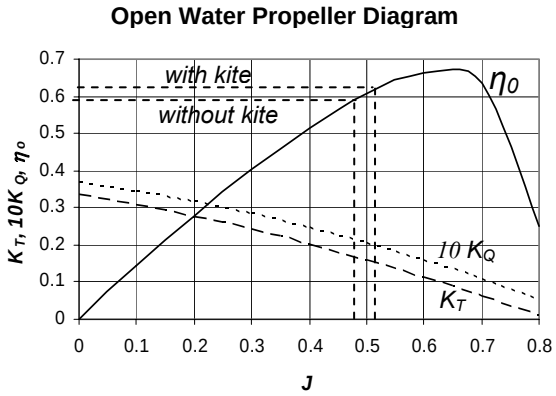

Figure 12, Open water propeller diagram

increase of 6.8 %. A similar effect was also mentioned by Molland [14]. The increase of open water efficiency appears to be much larger than the increase of brake specific fuel consumption (BSFC) of the engine for this case: the BSFC increases by 1.4 %.
Another expected unfavorable effect on the fuel consumption comes from the transverse force and resulting yaw moment induced by the kite. Due to this, a certain drift angle and rudder angle will be required to obtain force balance in transverse direction and yaw moment balance. Both will result in an increase of resistance.
Yaw balance is obtained by using the rudder. The rudder moment ($N_\delta \delta + N_{\delta\delta}\delta^2$ in equation (26)) and hydrodynamic moment on the hull ($N_v v$ in equation (26)) have opposite directions. From this it can be concluded that the optimal position to attach the kite is at the bow of the ship, thus minimizing the required rudder angle to obtain yaw balance. Doing so, the required rudder angles appeared not to exceed 4 degrees while the maximum drift angle amounts to less than 1 degree, resulting in a total maximum induced resistance due to drift and rudder angle of less than 1%.
Although no additional calculations have been carried out to prove this, the high efficiency of the hull is suspected to be caused by the fact that the forward ship speed is maintained when using the kite as auxiliary propulsion: far less favorable results are to be expected when the ship is driven by the kite alone resulting in a dramatic decrease of the forward speed.

The main conclusions summarized:

- Theoretical fuel saving for a 50.000 dwt tanker can amount to up to 50 % at Beaufort 7 with stern quartering wind using a kite of 500 m^2 attached to a 350 m towing line.

- Optimal flying altitude for the considered towing line lengths (150 m – 550 m) amounts to approx. 30 % of the towing line length
- Attaching the towing line to the bow minimizes required rudder angles.
- Losses due to drift, rudder angle and off design operation of the engine are small and counteracted by an improved open water propeller efficiency resulting in a relative fuel saving that roughly equals the relative traction force delivered by the kite.

3.6 FUTURE WORK

It should be noted that mentioned numbers of fuel saving correspond to certain environmental conditions. To say more about long term benefits, the percentage of occurrence of these condition during voyages has to be taken into account. Route optimization is expected to improve the economics of wind propulsion significantly. Voyage simulations should answer the question of how much can be gained in the long term.

The major uncertainties involved in the presented analysis are introduced by the calculation of the kite force. It is not known how valid the quasi-static approach is which is another reason to interpret presented fuel saving numbers carefully. Future work will concentrate on validation of the kite force calculation and/or using meaured kite forces [16] to perform the mentioned voyage simulations.

REFERENCES

[1] www.sustainableshipping.com
[2] www.skysails.com
[3] www.kiteship.com
[4] www.kiteboat.com
[5] Drela, M., Youngren, H., XFOIL 6.94 User Guide, MIT Dept. of Aerodynamica and & Astrodynamics, Aerocraft, Inc, 2001 (http://raphael.mit.edu/xfoil/xfoil_doc.txt)
[6] Drela, M.,An analysis and design system for low Reynold's number airfoils, MIT Dept. of Aerodynamica and & Astrodynamics,1989
[7] Troen, I. and Petersen, E.L., European Wind Atlas, Riso National Laboratory, 1989
[8] Lingard, J.S., Ram-air Parachute Design, Precision Aerial Delivery Seminar, 13th AIAA Aerodynamic Decelerator Systems Technology Conference, Clearwater Beach,1995
[9] Prakash, O., Aerodynamics and Longitudinal Stability of Parafoil/Payload System, Department of Aerospace Engineering, Indian Institute of Technology, Bombay, 2004
[10] Kleinwoud H., Stapersma D., Design of Propulsion and Electric Power Generation Systems, London, Imarest, 2003
[11] Journee J.M.J., Clarke D., Experimental Manoeuvring Data of Tanker "British Bombardier", Report No. 1429 Delft University of Technology Ship Hydromechanics Laboratory, Delft, 2005
[12] Naaijen P., Koster V., Dallinga R.P. On the Power Savings by an Auxiliary Kite Propulsion System, ISP Volume 53 No.4 2006
[13] Isherwood, R.M., Wind Resistance of Merchant Ships, Trans. of the Royal Institution of Naval Architects, 1973
[14] Molland, A.F., Operation of Propellers and Machinery in Wind Assisted Ships, Proc. of the First Wind Assisted Ship Propulsion Symposium, Glasgow, 1985
[15] A. Ilzhöfer, B. Lansdorp, M. Diehl, Results of optimisation of Laddermill sailing, to be published
[16] B. Lansdorp, R.Ruiterkamp, W.J. Ockels, Towards flight testing of remotely controlled surfkites for wind energy generation, Atmospheric Flight Mechanics Conference and Exhibit 2007, Hilton Head, USA, 2007